Development 135, 1647-1657 (2008) doi:10.1242/dev.020115

Live imaging of the *Dictyostelium* cell cycle reveals widespread S phase during development, a G2 bias in spore differentiation and a premitotic checkpoint

Tetsuya Muramoto and Jonathan R. Chubb*

The regulation of the *Dictyostelium* cell cycle has remained ambiguous owing to difficulties in long-term imaging of motile cells and a lack of markers for defining cell cycle phases. There is controversy over whether cells replicate their DNA during development, and whether spores are in G1 or G2 of the cell cycle. We have introduced a live-cell S-phase marker into *Dictyostelium* cells that allows us to precisely define cycle phase. We show that during multicellular development, a large proportion of cells undergo nuclear DNA synthesis. Germinating spores enter S phase only after their first mitosis, indicating that spores are in G2. In addition, we demonstrate that *Dictyostelium* heterochromatin is copied late in S phase and replicates via accumulation of replication factors, rather than recruitment of DNA to pre-existing factories. Analysis of variability in cycle times indicates that regulation of the cycle manifests at a single random transition in G2, and we present the first identified checkpoint in *Dictyostelium*, which operates at the G2–M transition in response to DNA damage.

KEY WORDS: Cell cycle, *Dictyostelium*, Checkpoint, Replication timing, PCNA

INTRODUCTION

Dynamic imaging of cell behaviour is crucial for understanding the regulation of the cell cycle. To define control points in the cell cycle requires knowledge of exactly where in the cycle a stimulus or stress elicits its effects. Imaging cells through whole cycles and identification of cycle position are necessary. The cell cycle of *Dictyostelium* has remained ambiguous largely owing to a lack of these imaging strategies. The normal control of the cell division cycle is unclear, and stress-induced checkpoints have not been identified. Many parental *Dictyostelium* cell lines have a high basal motility, preventing imaging of complete cycles. In addition, there are no markers to distinguish cycle phases in living cells. This has been unfortunate, as the relative developmental simplicity of the organism could potentially illuminate our understanding of the relationship between the cell cycle and differentiation. In addition, *Dictyostelium* has vertebrate DNA repair enzymes that are absent in yeast and invertebrate models, making it an excellent system for investigating relationships between DNA damage and the cell cycle (Hsu et al., 2006).

Growing *Dictyostelium* cells enter a differentiation programme upon starvation. After 6 hours of starvation, cells chemotax together to form a multicellular aggregate. This aggregate undergoes a series of morphogenetic transitions over the next 18 hours to form the mature fruiting body, composed of two major cell fates. Approximately 80% of cells form spores, suspended above the substrate by a stalk structure containing the remaining 20% of cells. During the cycle of growth and development, *Dictyostelium* cells are haploid.

Several studies suggest growing cells are predominantly in G2 phase of the cycle. The cell cycle status of differentiating cells is less clear. Several reports imply the decision to become stalk or spore is influenced by cycle phase before development, and that terminal differentiation occurs in G2 (Araki et al., 1994; Gomer and Firtel, 1987; MacWilliams et al., 2006; Maeda, 2005; McDonald and Durston, 1984; Weeks and Weijer, 1994; Weijer et al., 1984a; Weijer et al., 1984b). Cells grown on bacterial or glucose-free media as a food source are biased towards the stalk fate when mixed with cells grown in normal media (Leach et al., 1973; Thompson and Kay, 2000). One view is that the differentiation bias is caused by changes in cell cycle distribution in the population. There are conflicting reports about whether there is a G1 phase during differentiation. One view, based upon flow cytometric data of cellular DNA content, is that cells enter G1 prior to differentiation into stalks or spores (Chen and Kuspa, 2005; Chen et al., 2004). In addition, fluorescence in situ hybridisation (FISH) on hatching spores revealed one hybridisation signal, not two (Chen et al., 2004), supporting a G1 model. The other view, based upon direct fluorescence measurements of DAPI-stained nuclei, suggests spores have replicated DNA and are in G2 (MacWilliams et al., 2006; Weijer et al., 1984b).

Control points in the cell cycle are also undefined, although the *Dictyostelium* genome encodes homologues of many proteins implicated in cell cycle regulation in higher eukaryotes (Eichinger et al., 2005). An analysis of BrdU incorporation through development showed that reduced numbers of cells replicate their DNA during early starvation (Zimmerman and Weijer, 1993), followed by an increase in the proportion of cells undergoing replication after aggregate formation. These studies have been questioned, as nearly half of the cellular DNA is mitochondrial, and replication of this was proposed to contribute to the BrdU signal (Shaulsky and Loomis, 1995). It is also unclear to what extent cell division occurs during multicellular development. The cell cycle can be arrested in response to DNA-damaging agents, as exposure of cells to ultraviolet light reduces BrdU incorporation (Hoetzer and Deering, 1980; Ohnishi et al., 1981). However, the cycle stage(s) at which arrest occurs is not known. A recent study has identified *Dictyostelium* homologues of DNA repair factors previously unidentified outside vertebrates (Hudson et al., 2005). *Dictyostelium* has retained a homologue of DNA-PKcs (also known as Prkdc), a

Division of Cell and Developmental Biology, College of Life Sciences, University of Dundee, Dundee DD1 5EH, UK.

*Author for correspondence (e-mail: j.chubb@dundee.ac.uk)

Accepted 4 March 2008

component of the non-homologous end-joining (NHEJ) system. In vertebrates, this kinase is recruited to DNA ends by Ku proteins after double-strand breaks (DSBs). *Dictyostelium* cells lacking Ku or DNA-PKcs are defective in repair of DSBs, but only if breaks occur in spores (Hudson et al., 2005). This supported the idea that spores are in G1, since without a homologous template for homologous recombination, the NHEJ pathway would be required.

The ambiguities in the literature warrant a fresh approach. In *Dictyostelium*, imaging approaches have not been considered, as many parental strains have high motility. We have therefore used a parental cell line with low basal motility. This analysis was combined with a fluorescently tagged replication factor, proliferating cell nuclear antigen (PCNA), to mark S-phase cells (Leonhardt et al., 2000). This approach has enabled us to precisely define cell cycle phases in *Dictyostelium* during growth and development, and has illuminated the relationship between the cell cycle and development, the nature of normal cycle control and responsiveness of the cycle to sources of stress.

MATERIALS AND METHODS

Strains, growth and development

Strains were derived from the *Dictyostelium discoideum* AX2G (from J. G. Williams, University of Dundee, UK) grown in HL5 media (Sussman and Sussman, 1967) or on lawns of *Klebsiella aerogenes*. Development was initiated by washing cells twice in KK2 (20 mM potassium phosphate, pH 6.2) and plating on KK2 2% agar. After 5 minutes for cells to settle, buffer was removed and cells incubated at 22°C in a humidified chamber. AX2G was used because motility was lower (1.4 μm/minute) than other strains (AX3, 1.8 μm/minute; AX2, 5.2 μm/minute). AX2G had the lowest meandering index (displacement/distance covered; AX2G, 0.16; AX3, 0.27).

Generation of transgenic cell lines

To generate a construct for GFP-PCNA, we amplified and cloned the genomic PCNA sequence downstream of GFP into the *Eco*RI site of pDEXH82 (Konzok et al., 1999). Transformation was carried out as described (Muramoto et al., 2005). Selection of stable clones expressing GFP-PCNA used 10 μg/ml G418. Clones were maintained in 20 μg/ml G418. To express RFP-PCNA, the PCNA fragment from pDEXH82-GFP-PCNA was inserted downstream of RFP in pDEXHbsr. Selection was performed with 10 μg/ml blasticidin. To visualise nucleoli and heterochromatin, RFP-PCNA was co-expressed with eIF6-GFP (Balbo and Bozzaro, 2006) and GFP-HcpB (Kaller et al., 2006; Kaller et al., 2007). To express H2B-RFP, cells were transformed with a plasmid encoding mRFP-histone H2B (Fischer et al., 2004). The DNA-PKcs disruption construct contains bp 10417-11454 of the DNA-PKcs coding sequence followed by a blasticidin-resistance (bsr) cassette (Faix et al., 2004) then bp 14527-15624. The ku80 gene disruption construct contains bp –932 to –269 and 1307-2481 of the gene, with bsr intervening.

Fluorescence imaging of live cells

Prior to imaging, cells were plated on Lab-Tek chambered coverglass (Nunc) and incubated in 25% HL5/75% low fluorescence (LF) medium (Liu et al., 2002). Cells were imaged on an inverted Axiovert 200 microscope (Zeiss). Illumination was provided by a DG4 lamp (Sutter) through a GFP filter set (#41017, Chroma). To attenuate illumination we used a 0.6OD ND filter (Chroma) and reduced DG4 power to 33% of maximum. Cells were imaged with an ImagEM EM-CCD camera (C9100-13, Hamamatsu). The system was managed by Volocity Acquisition software (version 4.2, Improvision). Three-dimensional stacks were captured every 2.5 minutes with 330 nm *z*-steps and 30 millisecond exposures. We used a controllable XY stage with a piezo attachment for rapid 3D capture at multiple *xy* positions. For imaging 3-hour developed cells and slugs, squares of agar from development plates were excised and inverted onto Bioptechs Delta TPG dishes and covered with mineral oil to prevent desiccation. For imaging slugs, RFP-H2B/GFP-PCNA cells were mixed with untransformed AX2G cells at 1:9 ratio. Images were captured without prior fluorescence exposure, allowing blind capture. Bright-field illumination was used for focussing. Images are displayed as 2D projections of the original 3D stacks.

BrdU incorporation

Growth phase cells were cultured on μ-Dishes (Ibidi) with HL5 and labelled with 100 μM BrdU for 30 minutes. Fixation was carried out in ice-cold methanol containing 1% formaldehyde. GFP-PCNA images were captured from fields of cells at recorded stage positions. DNA was denatured in 2M HCl for 20 minutes before washing in PBS. BrdU was detected using anti-BrdU antibody (Roche) and Cy3 anti-mouse secondary (Jackson ImmunoResearch). Correlations between BrdU and PCNA were assessed by revisiting stage positions.

Spore germination

To activate germination, spores were resuspended in 20% DMSO in KK2 and incubated at 22°C for 1 hour. Spores were washed twice with KK2, incubated with 85 μl HL5, 255 μl LF and 40 μl heat-killed *Klebsiella* suspension on a μ-Dish, then imaged for 24 hours.

Bleomycin assays

Growth phase GFP-PCNA cells were plated on Lab-Tek coverglass at 5×10^5 cells/ml in 25% HL5/75% LF. During imaging, indicated concentrations of bleomycin sulphate (Sigma) were added. Washing out bleomycin comprised twice-repeated aspiration and replacement with fresh media.

RESULTS

A live-cell marker for the *Dictyostelium* cell cycle

Many DNA replication proteins have a punctate nuclear distribution during S phase, corresponding to sites of DNA replication, whilst having a nuclear diffuse distribution during G1 and G2 phases of the cell cycle (Aladjem, 2007; Leonhardt et al., 2000). In mammalian cells and yeast, fusion of GFP to PCNA can be used to follow the dynamics of these replication factories and their interaction with other nuclear components (Kitamura et al., 2006; Leonhardt et al., 2000; Meister et al., 2007).

We searched *Dictyostelium* sequence databases and identified an open reading frame (DDB0231779) with 57% identity to human PCNA. We made a GFP-PCNA fusion vector and expressed it in *Dictyostelium* parental cell lines. AX2G was selected for analysis as these cells have low basal motility, facilitating long-term imaging. The doubling time of GFP-PCNA cells in suspension culture was similar to the doubling time of other G418-resistant AX2G strains. The proportion of cells in S phase was similar in GFP-PCNA and parental cells, as assessed by BrdU incorporation.

GFP-PCNA has a characteristic dynamic distribution (Fig. 1A), revealed by time-lapse imaging of asynchronously growing cultures. The GFP-PCNA fluorescence was principally nuclear, with some cytoplasmic signal (Fig. 1A). We identified distinct nuclear patterns around mitosis. Prior to cell division, the nuclear-localised GFP-PCNA distributed all over the cell (*t*=–5:00 minutes), consistent with observations of a fenestrated mitosis in *Dictyostelium* (Moens, 1976). After cell division, GFP-PCNA rapidly accumulated on chromosomes to give a high intensity signal (*t*=0:00). As the nucleus expanded, weak foci became apparent (*t*=22:30). About 20 minutes after cell division, a single large bright spot was observed at the nuclear periphery (*t*=27:30, arrows, Fig. 1A). This persisted for 20 minutes then disappeared. The relative GFP-PCNA intensity of nucleus and cytoplasm changed around mitosis (Fig. 1B). The nuclear signal diminished during cell division, rapidly increased just after nuclear division, before decreasing gradually over the next 2-3 hours. Similar patterns of GFP-PCNA were observed in AX2 and AX3 parental strains (data not shown).

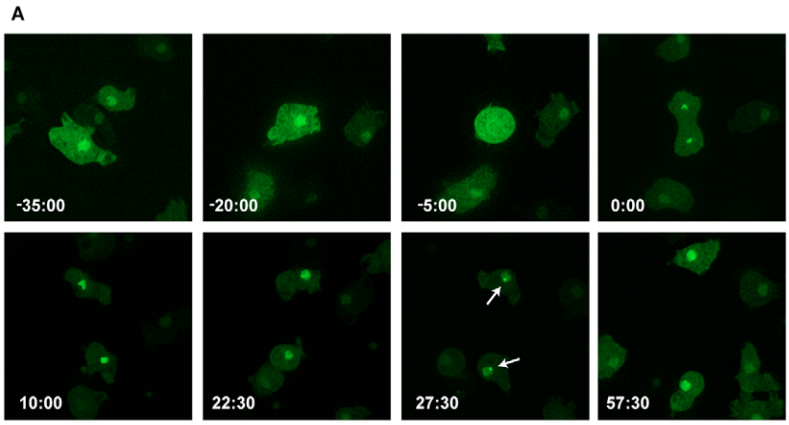

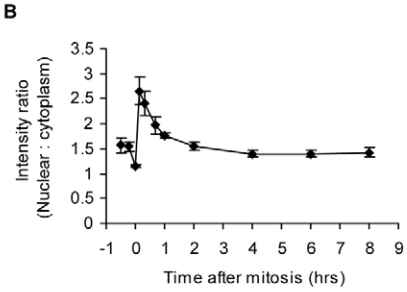

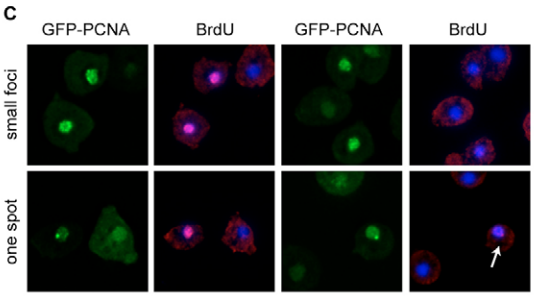

GFP-PCNA	BrdU	Cells
recruited to chromosomes	none	79 (100%)
	whole nucleus	0 (0%)
	spot	0 (0%)
small foci	none	50 (60%)
	whole nucleus	33 (40%)
	spot	0 (0%)
one spot	none	21 (15%)
	whole nucleus	109 (77%)
	spot	12 (8%)
no spot	none	
	whole nucleus	1
	spot	7

Fig. 1. Dynamic localisation of GFP-PCNA in *Dictyostelium* cells. (**A**) Localisation of GFP-PCNA during and after mitosis. Timing is in minutes relative to mitosis. Arrows indicate appearance of a nuclear peripheral GFP-PCNA spot. (**B**) Nuclear GFP-PCNA peaks after mitosis and decays in G2. Bars reflect s.d. (**C**) Comparison of BrdU incorporation (red) with GFP-PCNA localisation (green); DAPI (blue). Two examples are shown for small foci and one-spot nuclei. Arrow indicates a peripheral BrdU spot colocalised to the GFP-PCNA spot, as observed in a number of cells (see table).

We correlated GFP-PCNA distribution to DNA replication using BrdU incorporation (Fig. 1C). Cells finishing mitosis, with GFP-PCNA strongly recruited to chromosomes, did not stain positive for BrdU. Cells at the small foci stage had begun to show BrdU incorporation. Most cells with the single peripheral spot were BrdU positive. Indeed, some of these cells were seen to have a BrdU spot colocalising with the GFP-PCNA spot (arrow in Fig. 1C). Very few cells without PCNA spots incorporated BrdU. Given that BrdU incorporation is slow (incubation times shorter than 30 minutes were inefficient), these cells were likely to have just finished S phase, especially considering that most had the single peripheral BrdU spot, presumably late-replicating DNA. In summary, these data indicate that cells enter S phase a few minutes after chromosome segregation. This early phase of DNA replication manifests as a diffuse nuclear distribution of GFP-PCNA overlaid with weak foci. Cells then enter a late phase of DNA replication, dominated by the localisation of GFP-PCNA to a single spot.

To address the nature of the late-replicating chromatin, we co-expressed RFP-PCNA with the nucleolar marker eIF6-GFP (Balbo and Bozzaro, 2006), and the heterochromatin protein 1 (HP1) marker GFP-HcpB (Kaller et al., 2006). Two to four nucleoli are found per nucleus; however, these did not overlap with the PCNA spot (Fig. 2A). Instead, the RFP-PCNA spot colocalised to the GFP-HcpB spot. This implies that, as in mammalian cells, heterochromatin in *Dictyostelium* is late replicating. In both budding and fission yeast, heterochromatin is early replicating (Kim et al., 2003; Raghuraman et al., 2001).

Recent studies have considered the relative dynamics of chromatin and replication components (Kitamura et al., 2006; Meister et al., 2007; Sporbert et al., 2002). One view is that replication components move to chromatin, another is that chromatin is moved to pre-existing replication complexes. In mammalian cells, there is evidence that replication complexes move to adjacent chromatin by a domino-like effect (Sporbert et al., 2002). We addressed this issue for *Dictyostelium* heterochromatin by imaging S phase in cells co-expressing RFP-PCNA and GFP-HcpB (Fig. 2B). Heterochromatin foci were weak or absent during cell division, consistent with studies in mammalian cells demonstrating that HP1 disperses from chromatin at mitosis (Fischle et al., 2005). The heterochromatin spot reappeared within minutes after mitosis (t=5:00). During late S phase, the diffusely distributed PCNA was recruited to the pre-existing heterochromatin spot, while nucleoplasmic PCNA diminished (t=20:00). After S phase, PCNA dispersed, while the heterochromatin spot remained intact. Our data indicate that *Dictyostelium* heterochromatin is copied by the recruitment of replication factors, rather than by the heterochromatin being recruited to a preformed or adjacent factory.

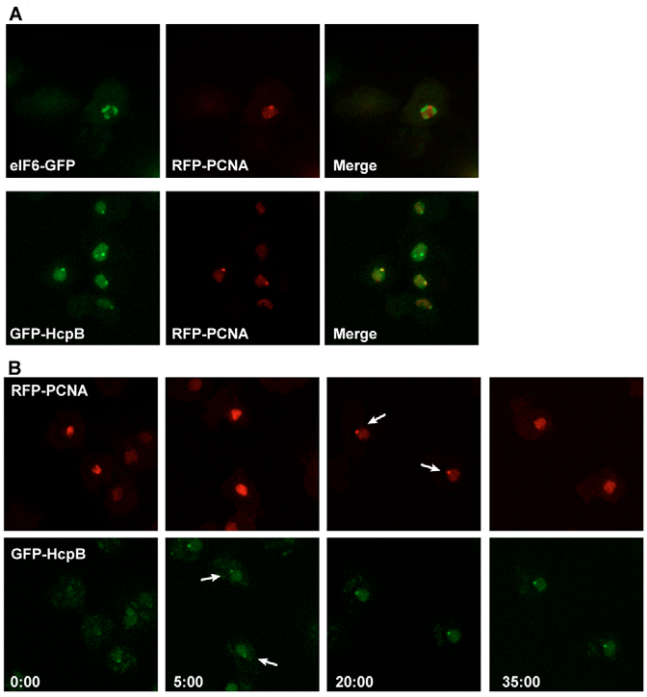

Fig. 2. *Dictyostelium* heterochromatin is late replicating. (**A**) Localisation of RFP-PCNA and heterochromatin (HcpB) and nucleolar (eIF6) markers. Right-hand panels show merged images. (**B**) Localisation of PCNA and HcpB after mitosis. The HcpB spot is assembled then recruits nucleoplasmic PCNA. Arrows indicate the times at which HcpB and PCNA spots become visible.

Timing and variability of the *Dictyostelium* cell cycle

Using a cell line of low motility expressing GFP-PCNA as an S-phase marker, we captured several hundred entire *Dictyostelium* cell cycles, an example of which is shown in Fig. 3. After mitosis and the short S phase, cells entered a long G2 (Figs 3 and 4). The mean length of mitosis was 5.5 minutes, early S was 21.5 minutes, and late S was 21.2 minutes (Fig. 4A). G2 was over 90% of the cell cycle, with an average length of 10.7 hours. All phases displayed considerable variability, although in absolute terms G2 accounted for almost all the heterogeneity in the *Dictyostelium* cell cycle. S-phase variance (55.75) contributed little to the overall variance (S+G2=19059). As the overall variance was not smaller than the sum of the individual variances in S and G2 (55.75+18675.51=18731.26), it appears that the timings of S and G2 are entirely independent, with no evidence of overlapping control processes. This contrasts with some mammalian cell lines, in which total cycle variance is less than the sum of the individual variances, implying overlapping control of phases (Brooks, 1981).

We found that sister cells had correlated G2 times when compared with randomly selected pairs. Sister cells did not usually divide synchronously, as evident from the sequence in Fig. 3; however, the difference in G2 times was smaller between sisters than between random pairs (see Fig. S1A in the supplementary material). When we plotted a frequency distribution for the time that cells remain in G2 after their sister has divided (the β curve), we obtained an exponential fit (Fig. 4B). This would be expected if the different division times of sister cells were the result of a single random transition (Brooks, 1981; Brooks et al., 1980).

S-phase timing was also correlated between sisters (Fig. 4C,D). For both early and late S, there was less variation in timing between sisters than between random pairs, implying that replication timing can be epigenetically transmitted. Furthermore, this effect can be inherited through an entire cycle, as we observed a strong correlation between S-phase duration and the length of the preceding S (see Fig. S1B in the supplementary material). Epigenetic effects are often conflated with chromatin modification, although as sister cells share cytoplasmic components, these might also contribute to the inherited effect.

The cell cycle in *Dictyostelium* development

It is unclear whether *Dictyostelium* cells replicate their nuclear DNA during development. To track the cell cycle in vivo during multicellular stages of *Dictyostelium* development, we co-expressed GFP-PCNA with RFP-histone H2B (Fischer et al., 2004). This allowed identification of mitotic cells under the more difficult imaging conditions of the multicellular stages. A typical movie sequence of cells in the slug phase of development is shown in Fig. 5. The central cell divides (arrows, *t*=0:00), daughters accumulate nuclear PCNA (*t*=2:30), and the daughter remaining in the field proceeds into S phase (arrow, *t*=75:00). This indicates nuclear DNA synthesis occurs during development.

Mitosis and early S phase were both twofold longer in slugs as compared with growing cells (Fig. 6A). By contrast, cells during early starvation (3 hours) were not significantly altered in the length of their mitosis or S phase (Fig. 6A). There was no evidence of a protracted G1 in slugs, as all dividing cells that could be imaged for 80 minutes acquired the characteristic late S-phase spot (*n*=11). It is unclear whether the extended period before the PCNA spot appears represents an alteration in timing of early DNA replication, or the emergence of a short G1 during development. It is conceivable that extended mitosis and early S reflect slower spindle function and re-establishment of nuclear architecture resulting from distortion caused by adjacent cells.

We then quantified the changing proportions of cells in S phase during development, by monitoring nuclear GFP-PCNA in cells from disassociated multicellular aggregates. After 3 hours of starvation, the proportion of S-phase cells had diminished by a third, implying that 50% more were in G2 (Fig. 6B). They were not in G1, as 3-hour cells had a normal length S phase immediately following mitosis (Fig. 6A). The proportion of S-phase cells diminished further by the time of aggregation (6 hours). The proportion increased again at 12 hours, to a level twofold higher than in asynchronous growth, as the aggregate became more compact and the tip formed. During fruiting body formation (18 hours), the proportion of cells in S declined to less than 1%. The developmental variation in the proportion of cells undergoing S phase that we observed was similar to the data obtained by Zimmerman and Weijer using BrdU incorporation (Zimmerman and Weijer, 1993), although doubts have been raised that BrdU incorporation during development might have resulted from mitochondrial rather than nuclear DNA synthesis (Shaulsky and Loomis, 1995). Our analysis is consistent with synthesis being nuclear. Our data indicate a delayed but synchronous replication of nuclear DNA around 12 hours of development. The delay could result from mechanical forces impeding cell division in early aggregates, an intracellular control point released at around 12 hours, or perhaps a resetting of many cells to early G2 at the onset of starvation.

We observed a clear demarcation of cell cycle phase between presumptive spore- and stalk-generating zones of slugs (Fig. 6C). The anterior of the slug (presumptive stalk) had a number of larger

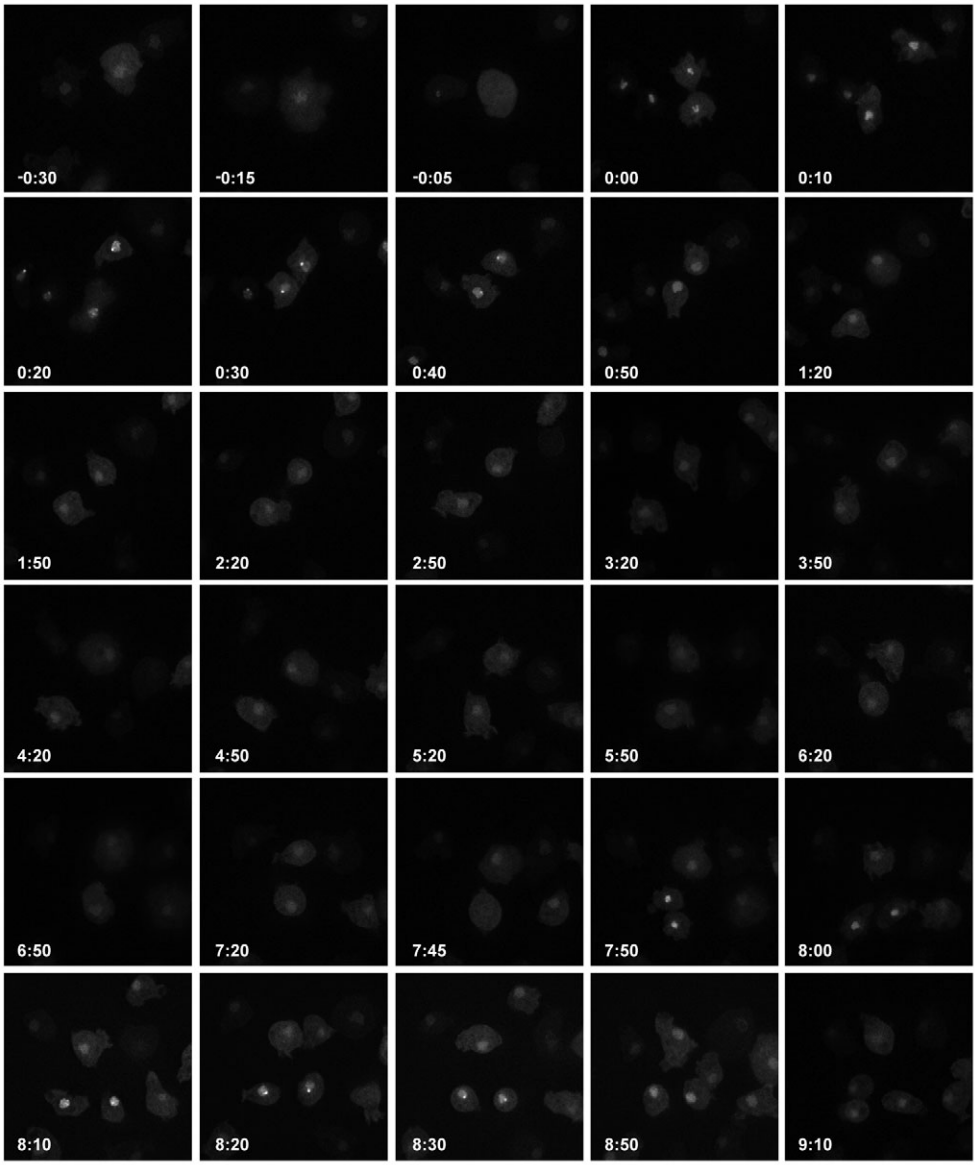

Fig. 3. Visualising the whole cell cycle of *Dictyostelium*. Cells expressing GFP-PCNA were imaged for complete cell cycles during asynchronous growth. Time (hours) from the first mitosis is indicated.

G2-like cells (large, with high cytoplasmic PCNA). Very few of these cells had clear GFP-PCNA spots. In the middle and posterior of the slug (presumptive spore), a high proportion of cells displayed either a bright spot or strong nuclear enrichment of GFP-PCNA, indicating a strong tendency of presumptive spore cells to replicate their nuclear DNA and enter G2.

The nutritional status of cells has been implicated in the regulation of cell fate choice, with cells grown on bacterial or glucose-free media as a food source having a greater tendency towards the stalk fate than those grown in normal media (Leach et al., 1973; Thompson and Kay, 2000). This has been proposed to result from alterations in the cell cycle. We addressed this by comparing cycles during growth in normal media, bacterial or glucose-free media. Cells grown without glucose had no change in S-phase length, although they appeared to have a slightly longer G2 (Fig. 6D). All cell cycle phases, except mitosis, were dramatically shorter during growth on bacteria. A link between nutrition and prestalk fate, occurring via cell cycle regulation, would therefore need to be different for different nutritional conditions. The surprising aspect of these data was the large difference in S-phase timing between growth on bacterial and normal media. A typical view of the mammalian somatic cell cycle is of cells reaching a transition point in G1, crossing this point then proceeding through S and G2 in a reasonably standard time. This would be expected to be condition dependent.

We now turn to the issue of whether *Dictyostelium* spores are in G1 or G2. Previous studies carried out on populations of germinating spores indicated that DNA replication and cell division occur from 20 hours after the beginning of germination (Chen et al., 2004). We repeated these experiments at single-cell resolution and observed a similar result. Fig. 7A shows that cells began DNA replication around 20 hours after germination, as assessed by the BrdU incorporation of individual cells. Fig. 7B shows that cells began dividing around the same time after germination, under similar culture conditions. By comparing BrdU incorporation using pulsed-field gels with cell division assessed by nuclear flow cytometry, Chen et al. inferred that S phase occurs before the first mitosis (Chen et al., 2004). However, on the basis of our single-cell analysis of BrdU incorporation and mitosis, this was not apparent, even though this approach is more direct. Therefore, to resolve the

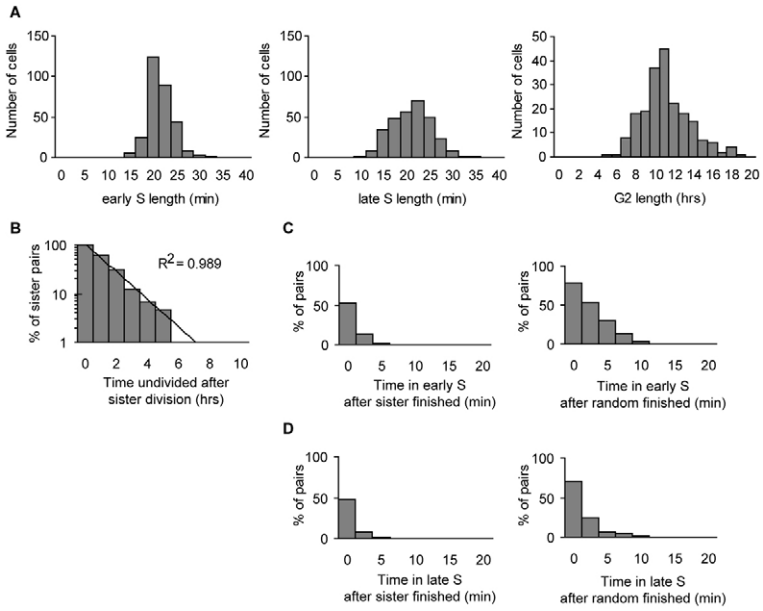

Fig. 4. Timing and variability of cell cycle phases. Cell cycle analysis was performed on whole cycles of *Dictyostelium* cells expressing GFP-PCNA, in asynchronous culture. (**A**) Distribution of cell cycle timing for early S, late S and G2. (**B**) Frequency distribution of G2 variation between sister cells, representing the time cells remain in G2 after their sister has divided. Includes exponential fit. (**C**,**D**) Frequency distributions of S variation between sisters, representing the time cells remain in early (C) or late (D) S phase after their sister has finished dividing. Random pair comparisons are shown on the right.

issue, we looked with greater resolution at the relative timing of these events using GFP-PCNA as a marker. All our movies showed that the characteristic GFP-PCNA distributions of S phase occur from about 20 hours after initiating germination; however, it is clear that the events of S phase occurred only after the first mitosis (Fig. 7C). Of the 20 cells we imaged before, during and after the first division, all completed mitosis before entering S phase, indicating that spores are in G2. It seems unlikely that an unusual spore chromosome configuration might mask a morphologically different S phase prior to mitosis, as normal heterochromatin foci were observed in germinating spores (see Fig. S2 in the supplementary material).

A *Dictyostelium* checkpoint

Previous reports suggested that DNA damage can stop cell growth and DNA replication in *Dictyostelium* (Hoetzer and Deering, 1980; Ohnishi et al., 1981); however, the point(s) in the cell cycle at which arrest occurs is undefined. With the ability to watch entire cycles and discriminate between different cycle phases, we have been able to do this.

We incubated GFP-PCNA-expressing cells in different concentrations of the DNA double-strand-break-inducing agent bleomycin (Chen and Stubbe, 2004). We carried out time-lapse imaging of cells before, during and after bleomycin treatment, and scored the number of cells undergoing mitosis per hour. The data for

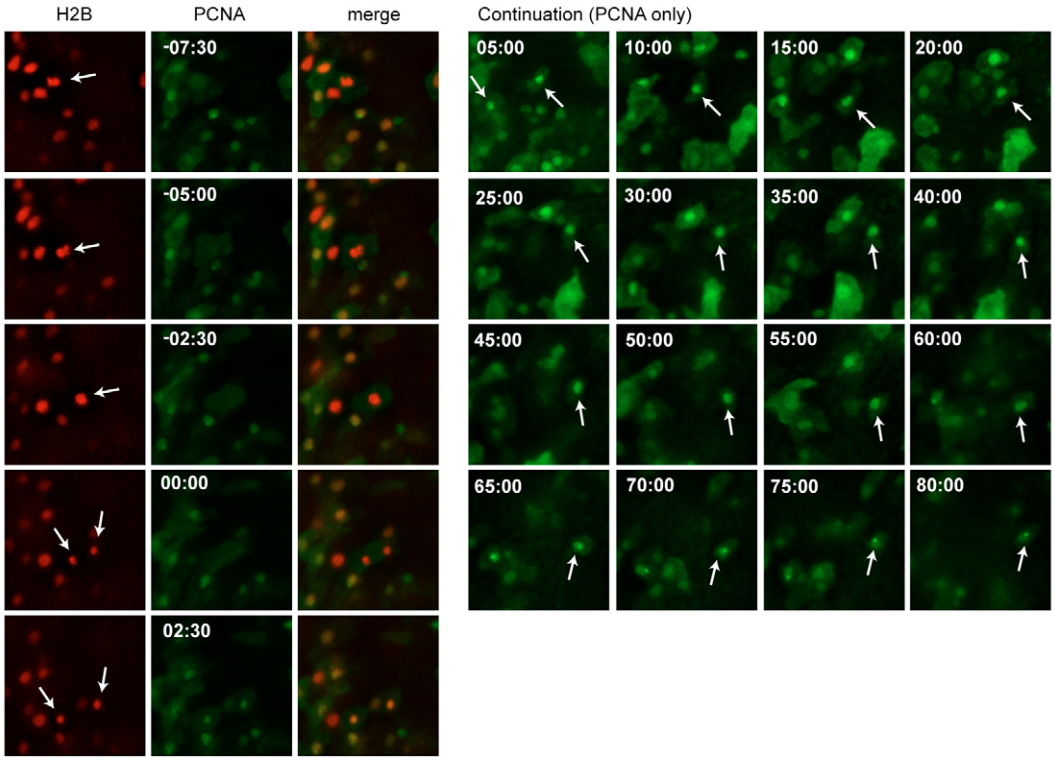

Fig. 5. Visualising mitosis and DNA replication in multicellular development. Mitotic cells were identified using RFP-H2B as a marker for chromatin. These cells were followed for up to 2 hours in the slug stage of development. GFP-PCNA was tracked to identify S-phase cells. The movie is of the prespore region of the slug. The first five frames include both RFP-H2B and GFP-PCNA. The RFP-H2B panels show a cell division in the central cell (arrows). The continuation of the movie (5:00 onwards), showing GFP-PCNA alone, allows one daughter cell (arrows) to be followed into S phase.

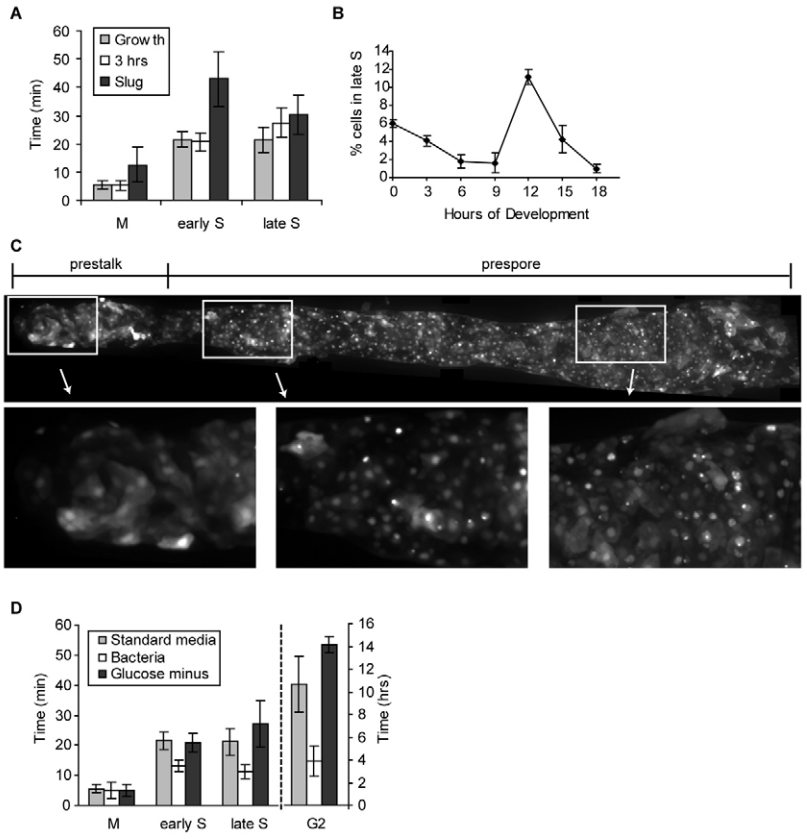

Fig. 6. Developmental regulation of the cell cycle. (**A**) Live-cell measurements of lengths of M, early and late S phases in growing (growth), 3-hour developed (3 hrs) and slug cells. Bars indicate s.d. (**B**) Developmental variation in the proportion of the population in late S phase. Snapshots were collected of cells at different stages in development, using disaggregated cells for multicellular stages. Bars represent s.d. (**C**) Reconstructed image of an intact slug showing S-phase distribution. S-phase cells are abundant in the middle and posterior of slugs (prespore fate). Few S-phase cells are observed in the anterior of slugs (prestalk fate). (**D**) Effects of nutrition on cycle phases. Cells were cultured in standard imaging media (25% HL5/75% LF), bacterial and glucose-free media (25% HL5/75% LF without glucose).

a typical experiment are shown in Fig. 8A. Without bleomycin, cells continued dividing for the whole movie. The number of cell divisions increased towards the end of the movie, as cell numbers increased. When low doses (5 mU/ml) of bleomycin were added, the effects on cell division were dramatic compared with the mild effect seen with mock treatment. Within 10-15 minutes of addition, all cell division had stopped. After 3 hours, the bleomycin was washed out. Five hours after the removal of bleomycin, a wave of cell division occurred in the population (Fig. 8A and images in Fig. 8B). These data are best explained by the presence of a DNA damage checkpoint operating at the G2–M transition in *Dictyostelium*. In response to DNA damage, cells accumulate at a point in the cell cycle just before mitosis. After breaks are repaired, cells re-enter the cycle with enhanced synchronicity. All arrested cells retained a nuclear enrichment of GFP-PCNA during bleomycin treatment, indicating that the checkpoint operates before nuclear envelope breakdown. We saw a similar response at a higher bleomycin dose (20 mU/ml; Fig. 8A). No cell death was seen at either 5 or 20 mU/ml bleomycin during the imaging period.

We then looked for evidence of an S-phase checkpoint. We concentrated on cells managing to divide during the first few minutes of bleomycin treatment. These cells exhibited the characteristic S-phase spots and became G2-phase cells. S-phase timing was slightly increased in 100 mU/ml (mean 56.07 minutes; s.d. 10.14) and 20 mU/ml (mean 50.97; s.d. 9.88) bleomycin as compared with untreated controls (mean 42.12; s.d. 5.48) (see Fig. S3B in the supplementary material). These results suggest that *Dictyostelium* S phase might be affected by DSBs, but, relative to the G2–M checkpoint, only modestly.

The *Dictyostelium* genome appears to encode many of the regulators of DNA damage responses known in vertebrates, including some absent from yeast and invertebrate models (Hsu et al., 2006). The genome encodes an ATM/ATR kinase-like molecule (Hurley and Bunz, 2007). In other systems, these enzymes phosphorylate histone variant H2AX at sites of DSBs, a crucial signalling event in the formation of repair complexes. The enzymes are essential in most systems, but can be inhibited by caffeine (Block et al., 2004; Sarkaria et al., 1999). Surprisingly, application of 1 mM caffeine impaired the ability of *Dictyostelium* to recover from bleomycin treatment (see Fig. S3A in the supplementary material). The frequency of dividing cells after bleomycin removal was greatly reduced. When 30 mM caffeine was administered during bleomycin treatment, no cells escaped the checkpoint to divide. However, an unusual response occurred; Fig. 9A shows two examples of this. The cells appeared to begin the mitotic programme, as the GFP-PCNA became dispersed throughout the cell. The GFP-PCNA was then recruited to chromosomes in the absence of cell division. This perhaps indicates some kind of 'mitotic catastrophe', with cells behaving as if in S phase after a failed division, perhaps resulting from failed checkpoint signalling. This behaviour was seen in 18 of 555 cells examined, but not in cells treated with either caffeine or bleomycin alone. These observations are consistent with a role for an ATM/ATR-like kinase in regulation of the *Dictyostelium* G2–M checkpoint.

The *Dictyostelium* genome encodes homologues of components of the non-homologous end-joining (NHEJ) machinery (Hudson et al., 2005). We investigated the role of two of these components, Ku and DNA-PKcs, in the DNA damage response of *Dictyostelium*. We disrupted the Ku and DNA-PKcs genes in GFP-PCNA cells by homologous recombination and imaged the mutant cells during and after bleomycin treatment (Fig. 9B). At 5 mU/ml bleomycin, both mutants arrested at the checkpoint. After bleomycin removal, cells began dividing again at a similar time to wild types. The recovery was not dramatically altered, although the DNA-PKcs null cells

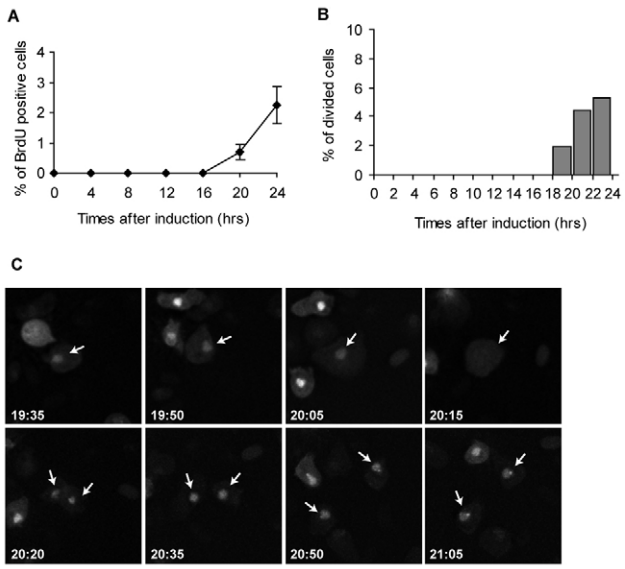

Fig. 7. Mitosis precedes S phase after spore germination. (**A**) Percentage of BrdU-positive cells after spore induction with DMSO; labelled with 100 μM BrdU for 30 minutes. Bars reflect s.d.; three replicates. (**B**) Onset of mitosis after spore germination. Percentage of cells dividing in 2-hour periods. First divisions occur in the 18-20 hour window. Two replicates. (**C**) Imaging-relative timing of division and S phase after spore germination, using GFP-PCNA as an S-phase marker. Stills from a movie of a germinated spore undergoing mitosis (arrows) are shown. Time after induction of germination (hours) is indicated.

displayed a marginal inhibition of division. At 20 mU/ml bleomycin, both mutants arrested normally, although their recovery was severely impaired. Cell division after bleomycin removal was delayed, and few cells divided during image capture. There was no evidence of cell death in the mutants, but during recovery, Ku and DNA-PKcs null cells displayed an unusual flattened morphology with high levels of cell motility (data not shown), indicating that the cells were under considerable stress. These data indicate that Ku and DNA-PKcs are active and necessary for a normal response to double-strand breaks in G2 in *Dictyostelium*. The mutants displayed no alteration in S-phase length (see Fig. S3B in the supplementary material): at both 20 and 100 mU/ml bleomycin, the length of S phase was similar to that of wild-type cells.

DISCUSSION

We have applied a fresh approach to the analysis of the *Dictyostelium* cell cycle. Using long-term imaging of living cells combined with a fluorescent S-phase marker, we have precisely defined the timing and variability of the different phases of the cycle. This has illuminated the control of the normal cycle, its regulation in development and its response to stress. Our approach will be of use in future investigations of the relationships between the cell cycle and cell and developmental processes.

Dictyostelium development and the cell cycle

Using GFP-PCNA as a marker, we have characterised developmental variation in the *Dictyostelium* cell cycle. We found an initial slowing of the cycle during the pre-aggregative phase of starvation, followed by a partially synchronous wave of S phase after aggregation. The cycle again subsided during fruiting body formation. We find no evidence of a prolonged G1 phase during development, as all cells that divided appeared to replicate their DNA within little more than an hour. By imaging the relative timing of cell division and S phase in hatching spores, we found that S phase does not occur until after the first division, implying that spores are predominantly in G2.

Several arguments initially supporting a G1 state in spores should be considered. Firstly, FISH reveals one spot of hybridisation in hatching spores, whereas in amoebae two spots are sometimes seen (Chen et al., 2004). In mammalian cells, this approach is not a reliable indicator of either G1 or G2, especially for heterochromatic sequences (Azuara et al., 2003). After DNA replication in eukaryotes, cohesin is loaded onto chromatin, which maintains sister chromatid pairing until anaphase (Nasmyth, 2005). Hence, fluorescently tagged DNA sequences in human cells usually reveal only a single spot until prophase (Thomson et al., 2004). Studies visualising transcription in living *Dictyostelium* cells revealed one spot in expressing cells, most of which should be in G2 (Chubb et al., 2006b). Not surprisingly, *Dictyostelium* has cohesin sequences in its genome. FISH requires DNA denaturation with formamide to allow probe access, but this can disrupt nuclear structure. In a spore, chromatin would be expected to be more compact, as spores are transcriptionally quiescent. Indeed, the preponderance of monomethylated over trimethylated lysine 4 of histone H3 in spores suggests a heterochromatic state (Chubb et al., 2006a). We propose that this state would be resistant to denaturation, and replicated loci would remain paired, as observed for heterochromatic loci in mammalian nuclei (Azuara et al., 2003).

The second argument supporting a G1 spore stems from flow cytometric data showing a decline in propidium iodide (PI) staining of cells during development (Chen et al., 2004). PI stains nucleic acids, but the conclusion that cellular DNA levels decline, and cells enter G1, presupposes DNA is equally accessible to PI during development. Quiescent chromatin during development could impede access of PI. Chen at al. raise this possibility and denatured cells with formamide to enhance access to DNA (Chen at al., 2004). However, as with FISH experiments, different chromatin states have different susceptibilities to denaturation. It is reasonable to assume that a decline of PI signal during development reflects closed chromatin, rather than a transition to G1.

Several studies have used BrdU incorporation to address whether cells replicate DNA and enter G2 during multicellular development. Using pulsed-field techniques, Chen et al. detected BrdU incorporation in only 2% of spore chromosomal DNA (Chen at al., 2004). Stronger incorporation was observed into mitochondrial DNA, as found previously (Shaulsky and Loomis, 1995), although labelling was considerably reduced relative to mitochondrial incorporation during growth. By contrast, Zimmerman and Weijer showed that a large proportion of prespore cells incorporate BrdU during development, as revealed by microscopy of fixed slugs (Zimmerman and Weijer, 1993), consistent with our data using a live-cell S-phase marker. How can these clear but opposing data be reconciled? Chen et al. argued that BrdU incorporation in multicellular aggregates reflects DNA repair or mitochondrial DNA replication (Chen et al., 2004), a view not supported by the data of Zimmerman and Weijer. BrdU incorporation observed in slugs appeared with a diffuse nuclear distribution, rather than the speckled distribution expected of mitochondria, including perinuclear mitochondria (van Es et al., 2001). The DNA repair model requires cell-type-specific synchronous nuclear-wide DNA damage, which seems unlikely.

Widespread S phase can clearly occur in multicellular development, but discrepancies suggest BrdU labelling during development is fickle, as also observed for tritiated thymidine (Zimmerman and

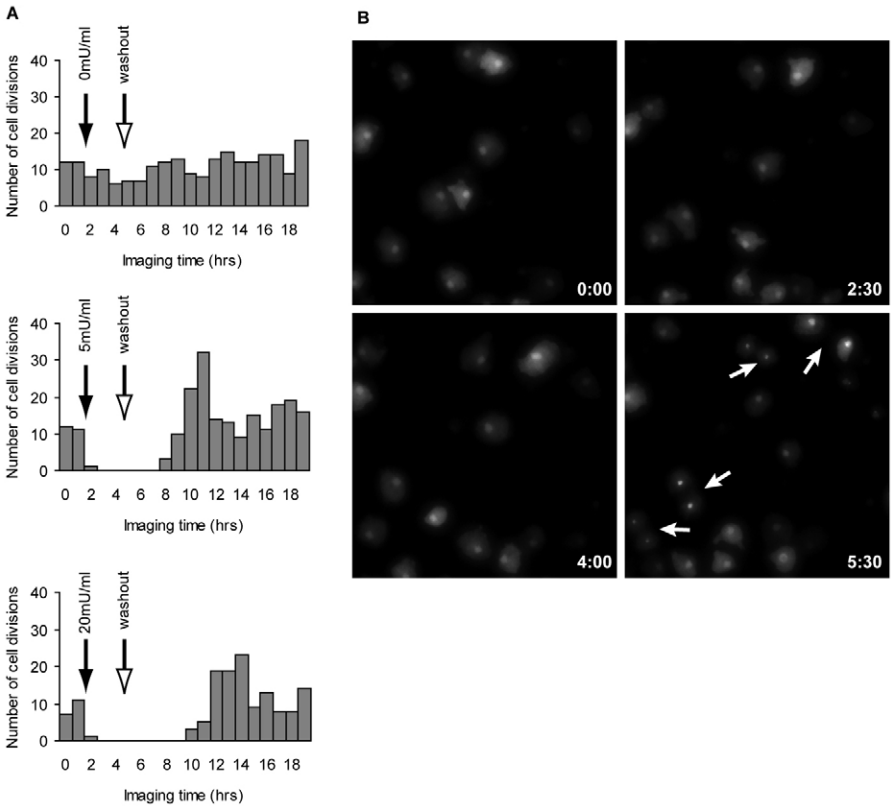

Fig. 8. Identification of a DNA damage checkpoint in *Dictyostelium*. (**A**) Cells were treated with bleomycin for 3 hours as indicated. The number of cell divisions occurring per hour was scored in mock-treated cells and those treated with 5 mU/ml or 20 mU/ml bleomycin. (**B**) After removal of bleomycin, cells escape the checkpoint and divide with increased synchronicity, as shown pictorially in these stills from a movie. Arrows indicate dividing cells.

Weijer, 1993). Differences in BrdU penetration are unlikely, as mitochondria incorporate BrdU even when nuclei cannot. Clearly, the two studies observed different things, albeit using different cell lines and labelling/detection techniques. It is conceivable that the cell lines differ in nucleotide biosynthesis pathway activities during development (Reome et al., 2000). Biosynthesis of dNTPs in the cytosol uses both nucleotide salvage and de novo synthesis pathways, whereas only the salvage pathway operates in mitochondria (Rampazzo et al., 2007). In mammalian cells, de novo dNTP biosynthesis components, such as ribonucleotide reductase, are induced at G1–S, satisfying dNTP demand (Magnusson et al., 2003). *Dictyostelium* ribonucleotide reductase is expressed during growth, repressed during starvation then strongly re-induced after aggregation in prespore cells (MacWilliams et al., 2001; Tsang et al., 1996),

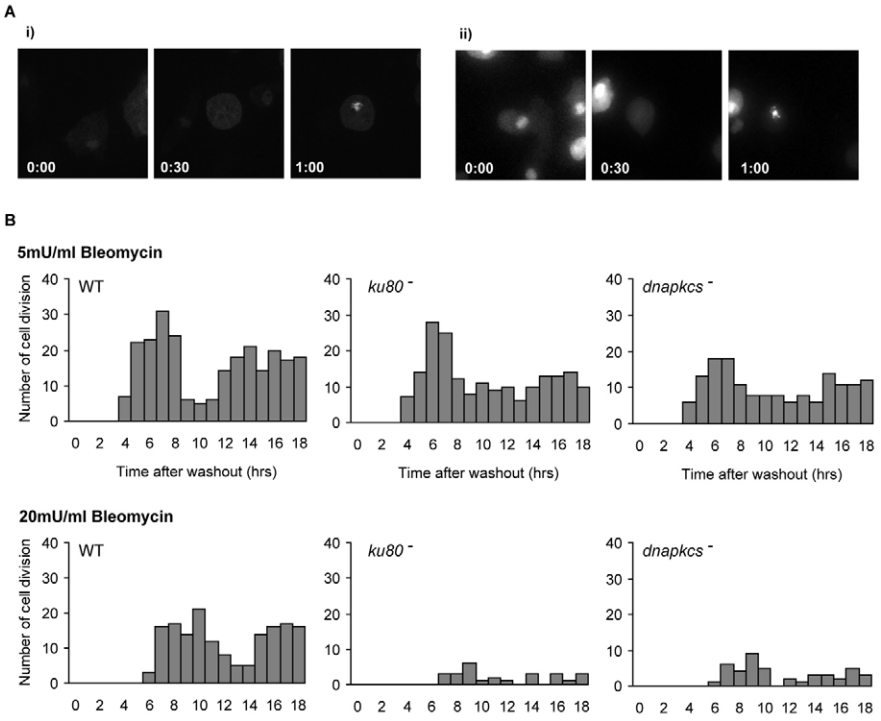

Fig. 9. Regulation of the DNA damage response. (**A**) Treatment of *Dictyostelium* cells with 30 mM caffeine and 20 mU/ml bleomycin causes a 'mitotic catastrophe' phenotype. Two examples (i,ii) are shown. Cells enter an S-like state without division. (**B**) Response of Ku and DNA-PKcs mutant cells to bleomycin. At 20 mU/ml bleomycin, the Ku and DNA-PKcs mutants are impaired in the recommencement of cell division after checkpoint arrest.

coincident with the widespread S phase we observed. BrdU is only incorporated via salvage pathways, perhaps making mitochondrial incorporation resilient, even if BrdU were out-competed in nuclei by de novo synthesised dTTP. There are negative effects of extreme BrdU exposure in many cell types and these may interfere with incorporation (Reome et al., 2000). Both the Zimmerman and Chen studies discussed above used BrdU incubation times and doses considerably greater than sufficient for labelling growing cells, potentially exacerbating differences between cell lines. However, using a marker detached from issues of penetration and in vivo metabolism applying to synthetic nucleosides, the occurrence of widespread S phase during multicellular development seems clear. The idea that developing cells undergo a widespread 'virtual' S phase, with PCNA foci but no replication, is unsupported by studies indicating that replication factory formation depends upon the initiation of DNA synthesis (Kitamura et al., 2006).

A few words should be said regarding the proposed role of the cell cycle in determining cell fate. Growth of cells on bacteria or in media lacking glucose causes a prestalk bias (Thompson and Kay, 2000). We find no simple evidence that this results from a specific bias in the cell cycle. Our data show that bacterial culture greatly shortens all cycle phases. By contrast, growth in media lacking glucose has little effect on cycles, beyond a small increase in G2 duration. Other features of these culture conditions might be important. Bacterial or glucose-free culture gives rise to smaller cells. These cells are more motile than those grown in normal media (Varnum et al., 1986) (data not shown). Both size and motility could influence the sorting of cells in aggregates. There might also be a direct effect of glucose levels.

Control points in the *Dictyostelium* cell cycle

Our analysis of the variability in G2 lengths between sister cells indicates that passage through cell cycles can be explained as a decision taken at a random transition point in G2, contrasting with the standard mammalian cycle in which the transition, referred to as a restriction point or G_0, occurs in G1. What is the nature of this transition point? Perhaps it is the opportunity for cells to assess whether they have grown enough to divide at a reasonable size, although strict size controls may not exist in all cell lines (Conlon and Raff, 2003). The transition probability should vary in different conditions. Firstly, cells grown on bacteria are smaller than cells in normal media, yet they have a shorter G2. In addition, cells accumulate in G2 during early starvation, implying that the transition threshold is elevated.

We have also defined a *Dictyostelium* DNA damage response checkpoint, which operates in late G2 and arrests cells in response to double-strand breaks. The NHEJ components Ku and DNA-PKcs were not required for checkpoint function, and at low bleomycin levels they were not necessary for recovery from the checkpoint, implying that the alternative repair pathway, homologous recombination, operates in their absence. However, at moderate bleomycin levels, Ku and DNA-PKcs were required for checkpoint recovery, implying NHEJ is active in G2, and can be necessary. The prevailing view is that homologous recombination operates in G2, where there is a template for repair, whereas NHEJ operates in G1, where there is no homologue. Our data indicate that this view is not absolute, and if cells are under considerable mutagenic stress then the homologous recombination pathway can be overloaded and NHEJ can help if required. An earlier study on *Dictyostelium* NHEJ mutant cells only found defects in spore viability (Hudson et al., 2005). Vegetative Ku and DNA-PKcs mutant cells recovered from DSBs as well as wild types. The defects we observed in the Ku and DNA-PKcs mutants might not be apparent in the plaque-formation viability assay of Hudson et al. Their work assessed survival and growth on bacterial lawns after mutagen treatment, whereas we studied acute recovery immediately after bleomycin removal. Short-term effects would be masked after several days of rapid growth on bacteria. Hudson et al. suggested that the spore defect reflected G1 spores (Hudson et al., 2005), whereas our data indicate that spores are in G2. However, we have shown that Ku and DNA-PKcs can function in G2, so a spore need not be in G1 to require NHEJ. A compelling alternative hypothesis is that NHEJ is required at high levels of DSBs in *Dictyostelium*. Stress on chromatin in generating and hatching a spore must be considerable, even without bleomycin. Condensation and decondensation are likely to require the making of DSBs by topoisomerases. Breaks in the inert environment of the spore might not be healed until germination, placing an instant high load on repair pathways. In the presence of additional mutagenic stress, NHEJ would surely be required to meet this load.

We thank Michelle Stevense for assistance with transformations, members of the *Dictyostelium* community for plasmids, our colleagues for comments on the paper and Dr Robert Brooks for assistance with cell cycle analysis. This work was supported by a MRC Career Development Award to J.R.C.

Supplementary material

Supplementary material for this article is available at http://dev.biologists.org/cgi/content/full/135/9/1647/DC1

References

Aladjem, M. I. (2007). Replication in context: dynamic regulation of DNA replication patterns in metazoans. *Nat. Rev. Genet.* **8**, 588-600.
Araki, T., Nakao, H., Takeuchi, I. and Maeda, Y. (1994). Cell-cycle-dependent sorting in the development of Dictyostelium cells. *Dev. Biol.* **162**, 221-228.
Azuara, V., Brown, K. E., Williams, R. R., Webb, N., Dillon, N., Festenstein, R., Buckle, V., Merkenschlager, M. and Fisher, A. G. (2003). Heritable gene silencing in lymphocytes delays chromatid resolution without affecting the timing of DNA replication. *Nat. Cell Biol.* **5**, 668-674.
Balbo, A. and Bozzaro, S. (2006). Cloning of Dictyostelium eIF6 (p27BBP) and mapping its nucle(ol)ar localization subdomains. *Eur. J. Cell Biol.* **85**, 1069-1078.
Block, W. D., Merkle, D., Meek, K. and Lees-Miller, S. P. (2004). Selective inhibition of the DNA-dependent protein kinase (DNA-PK) by the radiosensitizing agent caffeine. *Nucleic Acids Res.* **32**, 1967-1972.
Brooks, R. F. (1981). Random transitions and cell cycle control. *Prog. Clin. Biol. Res.* **66 Pt A**, 593-601.
Brooks, R. F., Bennett, D. C. and Smith, J. A. (1980). Mammalian cell cycles need two random transitions. *Cell* **19**, 493-504.
Chen, G. and Kuspa, A. (2005). Prespore cell fate bias in G1 phase of the cell cycle in Dictyostelium discoideum. *Eukaryot. Cell* **4**, 1755-1764.
Chen, G., Shaulsky, G. and Kuspa, A. (2004). Tissue-specific G1-phase cell-cycle arrest prior to terminal differentiation in Dictyostelium. *Development* **131**, 2619-2630.
Chen, J. and Stubbe, J. (2004). Bleomycins: new methods will allow reinvestigation of old issues. *Curr. Opin. Chem. Biol.* **8**, 175-181.
Chubb, J. R., Bloomfield, G., Xu, Q., Kaller, M., Ivens, A., Skelton, J., Turner, B. M., Nellen, W., Shaulsky, G., Kay, R. R. et al. (2006a). Developmental timing in Dictyostelium is regulated by the Set1 histone methyltransferase. *Dev. Biol.* **292**, 519-532.
Chubb, J. R., Trcek, T., Shenoy, S. M. and Singer, R. H. (2006b). Transcriptional pulsing of a developmental gene. *Curr. Biol.* **16**, 1018-1025.
Conlon, I. and Raff, M. (2003). Differences in the way a mammalian cell and yeast cells coordinate cell growth and cell-cycle progression. *J. Biol.* **2**, 7.
Eichinger, L., Pachebat, J. A., Glockner, G., Rajandream, M. A., Sucgang, R., Berriman, M., Song, J., Olsen, R., Szafranski, K., Xu, Q. et al. (2005). The genome of the social amoeba Dictyostelium discoideum. *Nature* **435**, 43-57.
Faix, J., Kreppel, L., Shaulsky, G., Schleicher, M. and Kimmel, A. R. (2004). A rapid and efficient method to generate multiple gene disruptions in Dictyostelium discoideum using a single selectable marker and the Cre-loxP system. *Nucleic Acids Res.* **32**, e143.
Fischer, M., Haase, I., Simmeth, E., Gerisch, G. and Muller-Taubenberger, A. (2004). A brilliant monomeric red fluorescent protein to visualize cytoskeleton dynamics in Dictyostelium. *FEBS Lett.* **577**, 227-232.
Fischle, W., Tseng, B. S., Dormann, H. L., Ueberheide, B. M., Garcia, B. A., Shabanowitz, J., Hunt, D. F., Funabiki, H. and Allis, C. D. (2005). Regulation of HP1-chromatin binding by histone H3 methylation and phosphorylation. *Nature* **438**, 1116-1122.

Gomer, R. H. and Firtel, R. A. (1987). Cell-autonomous determination of cell-type choice in Dictyostelium development by cell-cycle phase. *Science* **237**, 758-762.
Hoetzer, K. E. and Deering, R. A. (1980). Sensitization of rad mutants of Dictyostelium discoideum to ultraviolet light by postirradiation treatment with caffeine. *Mutat. Res.* **71**, 273-276.
Hsu, D. W., Gaudet, P., Hudson, J. J., Pears, C. J. and Lakin, N. D. (2006). DNA damage signaling and repair in Dictyostelium discoideum. *Cell Cycle* **5**, 702-708.
Hudson, J. J., Hsu, D. W., Guo, K., Zhukovskaya, N., Liu, P. H., Williams, J. G., Pears, C. J. and Lakin, N. D. (2005). DNA-PKcs-dependent signaling of DNA damage in Dictyostelium discoideum. *Curr. Biol.* **15**, 1880-1885.
Hurley, P. J. and Bunz, F. (2007). ATM and ATR: components of an integrated circuit. *Cell Cycle* **6**, 414-417.
Kaller, M., Euteneuer, U. and Nellen, W. (2006). Differential effects of heterochromatin protein 1 isoforms on mitotic chromosome distribution and growth in Dictyostelium discoideum. *Eukaryot. Cell* **5**, 530-543.
Kaller, M., Foldesi, B. and Nellen, W. (2007). Localization and organization of protein factors involved in chromosome inheritance in Dictyostelium discoideum. *Biol. Chem.* **388**, 355-365.
Kim, S. M., Dubey, D. D. and Huberman, J. A. (2003). Early-replicating heterochromatin. *Genes Dev.* **17**, 330-335.
Kitamura, E., Blow, J. J. and Tanaka, T. U. (2006). Live-cell imaging reveals replication of individual replicons in eukaryotic replication factories. *Cell* **125**, 1297-1308.
Konzok, A., Weber, I., Simmeth, E., Hacker, U., Maniak, M. and Muller-Taubenberger, A. (1999). DAip1, a Dictyostelium homologue of the yeast actin-interacting protein 1, is involved in endocytosis, cytokinesis, and motility. *J. Cell Biol.* **146**, 453-464.
Leach, C. K., Ashworth, J. M. and Garrod, D. R. (1973). Cell sorting out during the differentiation of mixtures of metabolically distinct populations of Dictyostelium discoideum. *J. Embryol. Exp. Morphol.* **29**, 647-661.
Leonhardt, H., Rahn, H. P., Weinzierl, P., Sporbert, A., Cremer, T., Zink, D. and Cardoso, M. C. (2000). Dynamics of DNA replication factories in living cells. *J. Cell Biol.* **149**, 271-280.
Liu, T., Mirschberger, C., Chooback, L., Arana, Q., Dal Sacco, Z., MacWilliams, H. and Clarke, M. (2002). Altered expression of the 100 kDa subunit of the Dictyostelium vacuolar proton pump impairs enzyme assembly, endocytic function and cytosolic pH regulation. *J. Cell Sci.* **115**, 1907-1918.
MacWilliams, H., Gaudet, P., Deichsel, H., Bonfils, C. and Tsang, A. (2001). Biphasic expression of rnrB in Dictyostelium discoideum suggests a direct relationship between cell cycle control and cell differentiation. *Differentiation* **67**, 12-24.
MacWilliams, H., Doquang, K., Pedrola, R., Dollman, G., Grassi, D., Peis, T., Tsang, A. and Ceccarelli, A. (2006). A retinoblastoma ortholog controls stalk/spore preference in Dictyostelium. *Development* **133**, 1287-1297.
Maeda, Y. (2005). Regulation of growth and differentiation in Dictyostelium. *Int. Rev. Cytol.* **244**, 287-332.
Magnusson, J., Orth, M., Lestienne, P. and Taanman, J. W. (2003). Replication of mitochondrial DNA occurs throughout the mitochondria of cultured human cells. *Exp. Cell Res.* **289**, 133-142.
McDonald, S. A. and Durston, A. J. (1984). The cell cycle and sorting behaviour in Dictyostelium discoideum. *J. Cell Sci.* **66**, 195-204.
Meister, P., Taddei, A., Ponti, A., Baldacci, G. and Gasser, S. M. (2007). Replication foci dynamics: replication patterns are modulated by S-phase checkpoint kinases in fission yeast. *EMBO J.* **26**, 1315-1326.
Moens, P. B. (1976). Spindle and kinetochore morphology of Dictyostelium discoideum. *J. Cell Biol.* **68**, 113-122.
Muramoto, T., Takeda, S., Furuya, Y. and Urushihara, H. (2005). Reverse genetic analyses of gamete-enriched genes revealed a novel regulator of the cAMP signaling pathway in Dictyostelium discoideum. *Mech. Dev.* **122**, 733-743.
Nasmyth, K. (2005). How might cohesin hold sister chromatids together? *Philos. Trans. R. Soc. Lond. B Biol. Sci.* **360**, 483-496.
Ohnishi, T., Okaichi, K., Ohashi, Y. and Nozu, K. (1981). Effects of caffeine on DNA repairs of UV-irradiated Dictyostelium discoideum. *Photochem. Photobiol.* **33**, 79-83.
Raghuraman, M. K., Winzeler, E. A., Collingwood, D., Hunt, S., Wodicka, L., Conway, A., Lockhart, D. J., Davis, R. W., Brewer, B. J. and Fangman, W. L. (2001). Replication dynamics of the yeast genome. *Science* **294**, 115-121.
Rampazzo, C., Fabris, S., Franzolin, E., Crovatto, K., Frangini, M. and Bianchi, V. (2007). Mitochondrial thymidine kinase and the enzymatic network regulating thymidine triphosphate pools in cultured human cells. *J. Biol. Chem.* **282**, 34758-34769.
Reome, J. B., Johnston, D. S., Helmich, B. K., Morgan, T. M., Dutton-Swain, N. and Dutton, R. W. (2000). The effects of prolonged administration of 5-bromodeoxyuridine on cells of the immune system. *J. Immunol.* **165**, 4226-4230.
Sarkaria, J. N., Busby, E. C., Tibbetts, R. S., Roos, P., Taya, Y., Karnitz, L. M. and Abraham, R. T. (1999). Inhibition of ATM and ATR kinase activities by the radiosensitizing agent, caffeine. *Cancer Res.* **59**, 4375-4382.
Shaulsky, G. and Loomis, W. F. (1995). Mitochondrial DNA replication but no nuclear DNA replication during development of Dictyostelium. *Proc. Natl. Acad. Sci. USA* **92**, 5660-5663.
Sporbert, A., Gahl, A., Ankerhold, R., Leonhardt, H. and Cardoso, M. C. (2002). DNA polymerase clamp shows little turnover at established replication sites but sequential de novo assembly at adjacent origin clusters. *Mol. Cell* **10**, 1355-1365.
Sussman, R. and Sussman, M. (1967). Cultivation of Dictyostelium discoideum in axenic medium. *Biochem. Biophys. Res. Commun.* **29**, 53-55.
Thompson, C. R. and Kay, R. R. (2000). Cell-fate choice in Dictyostelium: intrinsic biases modulate sensitivity to DIF signaling. *Dev. Biol.* **227**, 56-64.
Thomson, I., Gilchrist, S., Bickmore, W. A. and Chubb, J. R. (2004). The radial positioning of chromatin is not inherited through mitosis but is established de novo in early G1. *Curr. Biol.* **14**, 166-172.
Tsang, A., Bonfils, C., Czaika, G., Shtevi, A. and Grant, C. (1996). A prespore-specific gene of Dictyostelium discoideum encodes the small subunit of ribonucleotide reductase. *Biochim. Biophys. Acta* **1309**, 100-108.
van Es, S., Wessels, D., Soll, D. R., Borleis, J. and Devreotes, P. N. (2001). Tortoise, a novel mitochondrial protein, is required for directional responses of Dictyostelium in chemotactic gradients. *J. Cell Biol.* **152**, 621-632.
Varnum, B., Edwards, K. B. and Soll, D. R. (1986). The developmental regulation of single-cell motility in Dictyostelium discoideum. *Dev. Biol.* **113**, 218-227.
Weeks, G. and Weijer, C. J. (1994). The Dictyostelium cell cycle and its relationship to differentiation. *FEMS Microbiol. Lett.* **124**, 123-130.
Weijer, C. J., Duschl, G. and David, C. N. (1984a). Dependence of cell-type proportioning and sorting on cell cycle phase in Dictyostelium discoideum. *J. Cell Sci.* **70**, 133-145.
Weijer, C. J., Duschl, G. and David, C. N. (1984b). A revision of the Dictyostelium discoideum cell cycle. *J. Cell Sci.* **70**, 111-131.
Zimmerman, W. and Weijer, C. J. (1993). Analysis of cell cycle progression during the development of Dictyostelium and its relationship to differentiation. *Dev. Biol.* **160**, 178-185.

(A)

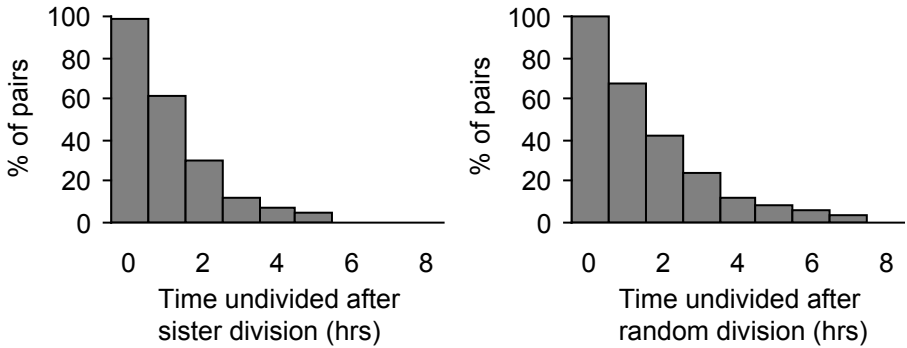
% of pairs
100
80
60
40
20
0
0
2
4
6
8
Time undivided after sister division (hrs)
% of pairs
100
80
60
40
20
0
0
2
4
6
8
Time undivided after random division (hrs)

(B)

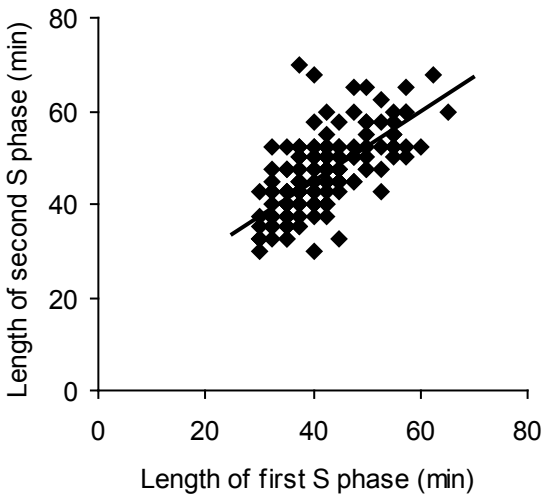
Length of second S phase (min)
80
60
40
20
0
0
20
40
60
80
Length of first S phase (min)

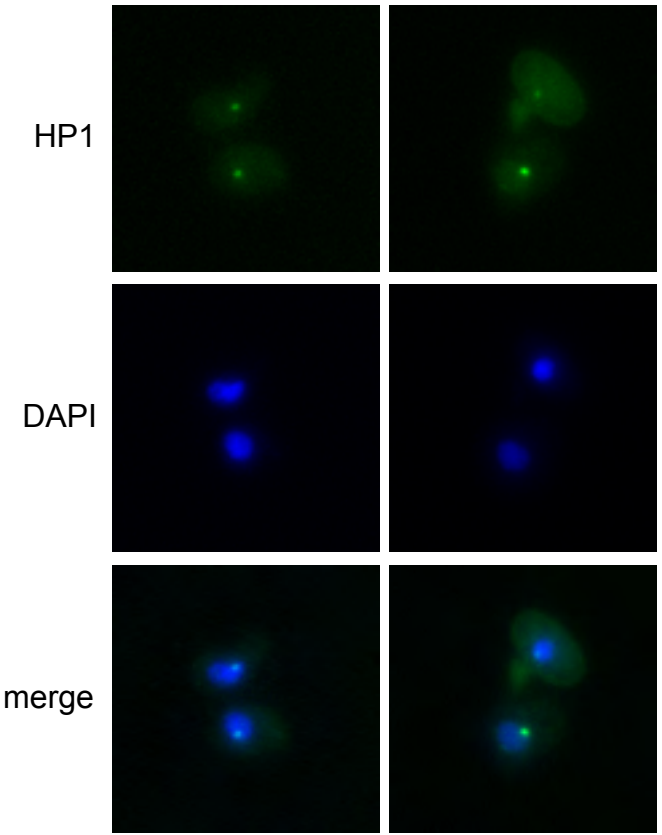
HP1
DAPI
merge

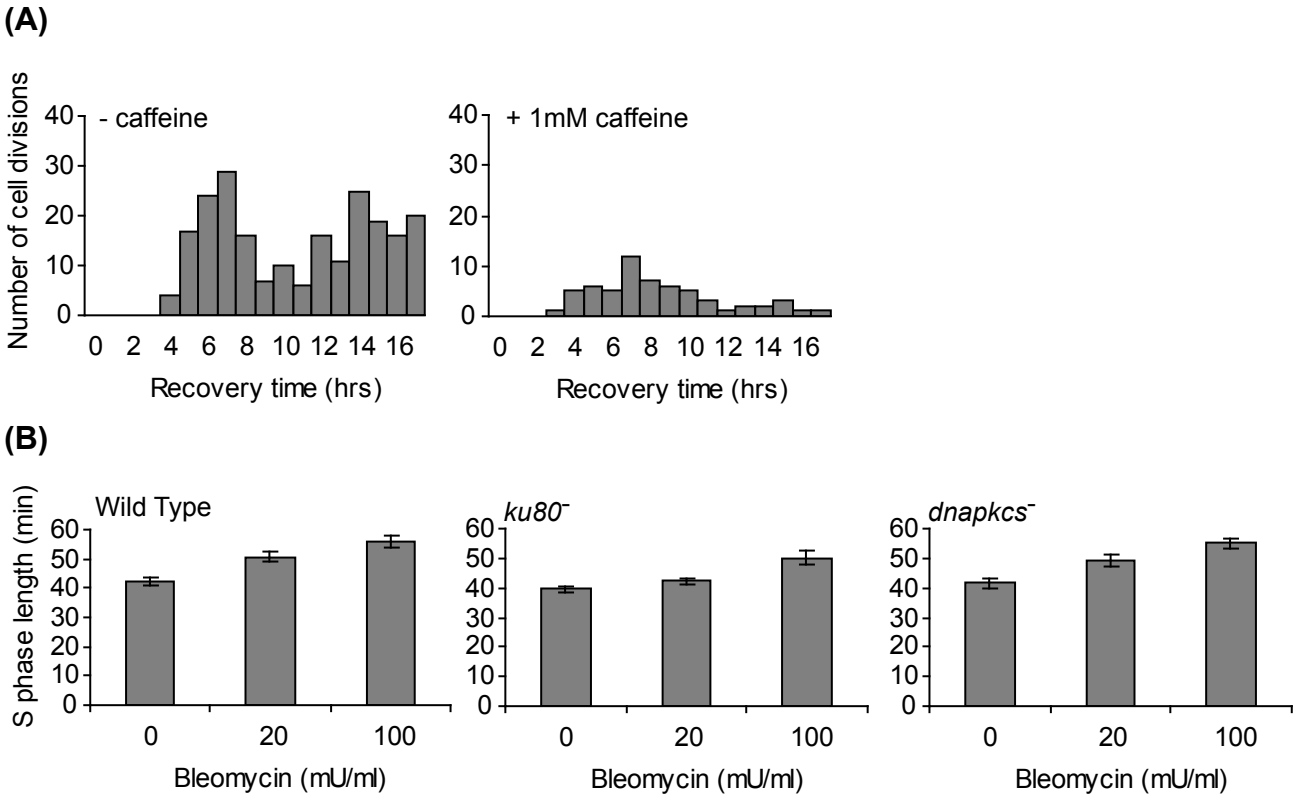
(A)
Number of cell divisions
- caffeine
+ 1mM caffeine
Recovery time (hrs)
Recovery time (hrs)
(B)
S phase length (min)
Wild Type
ku80⁻
dnapkcs⁻
Bleomycin (mU/ml)
Bleomycin (mU/ml)
Bleomycin (mU/ml)